

**Microwave Resonators and Filters**

**Daniel E. Oates**

**MIT Lincoln Laboratory**

**244 Wood St.**

**Lexington, MA 02478**

**USA**

**Email: [oates@ll.mit.edu](mailto:oates@ll.mit.edu)**

**Distribution A: Public Release**

This work is sponsored by the Naval Surface Warfare Center, Carderock Division under Air Force Contract #FA8721-05-C-0002. Opinions, interpretations, conclusions, and recommendations are those of the authors and are not necessarily endorsed by the United States Government.

## Equation Chapter 1 Section 1 Introduction

Why use superconductors? Although superconductors have zero resistance at DC, at any finite frequency the resistance is finite due to the presence of quasiparticles, which only vanish at zero temperature. As explained in other chapters, the surface resistance of superconductors at microwave frequencies can be as much as three orders of magnitude lower than the best normal metals such as copper, even at comparably low temperatures. This leads to resonators and filters with very low dissipation. The motivation for the use of superconductors in many applications, such as in high performance filters, is low loss even in a very small size. The energy stored is proportional to the volume occupied and the energy dissipated is proportional to the surface area. Since the  $Q$  of a circuit is the ratio of energy stored to energy dissipated per cycle, by making circuits arbitrarily large the  $Q$  can be made as large as possible even with normal conducting materials. Superconductors, however, can achieve high  $Q$  values even a small volume.

However superconductors also have additional unique properties, specifically kinetic inductance and nonlinearity that are exploited in applications other than filters. A word on kinetic inductance (Van Duzer and Turner 1999): it is a consequence of the zero resistance of a superconductor, in which energy can be stored in the kinetic energy of the current, in addition to the energy stored in the magnetic fields of the circuit. A normal conductor does not have kinetic inductance because energy cannot be stored in the current, which due to resistance, decays while a superconductor displays persistent currents. The kinetic inductance is electrically identical to the magnetic inductance and simply adds to the total inductance of the circuit. The ratio of kinetic inductance to magnetic inductance can vary greatly depending on the geometry of the device.

Changes in kinetic inductance due to increases in quasiparticle density in low-loss high- $Q$  resonators are used to realize sensitive radiation detectors. The details are discussed below. The interaction of superconducting resonators with qubits is used in quantum computing to detect the quantum state of the qubit, also discussed in this chapter.

The chapter on applications of superconducting resonators and filters in the first edition of this handbook (Z.-Y. Shen 2003) discussed the then state of the art of microwave frequency applications mostly using high-temperature superconductors (HTS). The fundamentals of filter design and operation remain unchanged so it is unnecessary to repeat them. This chapter will attempt to address more recent developments in filter applications. Many important new applications of microwave resonators are using low-temperature superconductors often coupled with systems already operating at low temperatures such as quantum information processing systems.

To put the applications discussed herein in proper context, the operating frequencies, temperatures, and power levels need to be quantified. In considering loss, the advantages of superconductors are greatest at frequencies below about 50 GHz. See Figure 1. Because the surface resistance of superconductors increases proportional to  $f^2$  and that of normal conductors as  $f^{1/2}$ , the advantage of superconductors over normal metals is greatest at microwave frequencies and below. The frequencies of operation are limited to approximately 50 GHz or below to maintain the large advantage over conventional materials. However, when  $\hbar\omega$  becomes greater than the superconducting energy gap  $\Delta$ , the radiation breaks pairs and losses increase sharply. For niobium for instance this is  $\sim 100$  GHz.

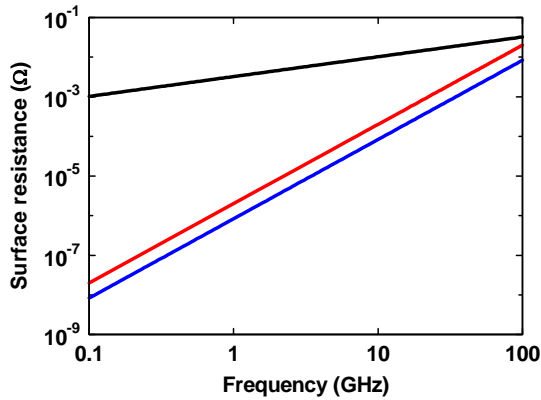


Figure 1 Surface resistance vs frequency Black: copper at 77 K  $\sim \sqrt{f}$  Red: YBCO at 77 K or Niobium at 7.7K  $\sim f^{1/2}$  Blue: YBCO at 40 K or Niobium at 4 K  $\sim f$

The operating temperatures fall into either of two ranges, 70-77 K for high-temperature superconductors (HTS) and 4 K or below for low-temperature superconductors (LTS). Although some HTS cuprate superconductors have  $T_c > 130$  K, only rare-earth barium copper oxide  $\text{ReB}_2\text{Cu}_3\text{O}_{7x}$  (ReBCO) where Re stands for a rare-earth element such as yttrium, YBCO, with  $T_c \approx 91$  K. has proven practical among the HTS materials. For LTS temperatures are usually 4 K or lower, 4 K for niobium and lower for other materials. Superconductors are limited in the amount of power that can be handled, because they are limited by critical currents and in the microwave region by flux penetration. The exact value of power handling is strongly dependent on the geometry and is limited to a few watts at most. This is discussed further in Section 3.3.

This chapter will be concerned with “electronic” applications of resonators and filters. Cavities fabricated from bulk materials are the state of the art for linear accelerators, but will not be treated here. For more detail see (Vaglio 2001)

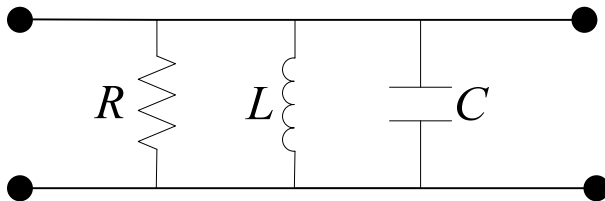


Figure 2 Equivalent circuit for a resonator.  $f_0 = \sqrt{1/LC}$  and  $Q = R/\omega L$

## 1. Resonators

### 1.1. Resonator basics

First we discuss resonators. Most superconducting filters are implemented with coupled resonators. Thus the resonator is basic to both filter and resonator applications. Microwave resonators are treated in many textbooks for example (Pozar 1998). Here some basics relevant to superconducting resonators are

reviewed. Figure 2 shows a convenient circuit model of a resonator, a parallel R-L-C circuit. Resonators are characterized by the resonant frequency  $f_0$  and quality factor  $Q$ . The  $Q$  is defined as

$$Q = 2\pi \frac{\text{Energy stored}}{\text{Energy lost per cycle}} \quad (1)$$

Where the denominator is the total energy lost including energy dissipated in the resonator due to resistive losses, energy lost (dissipated) to the environment such as circuits connected to the resonator, radiation, and spurious losses. It is usual to separate the dissipation internal to the resonator and the dissipation to the external circuits. Thus the measured quality factor  $Q_m$  is given by

$$\frac{1}{Q_m} = \frac{1}{Q_i} + \frac{1}{Q_c} \quad (2)$$

where  $Q_i$ , sometimes denoted as  $Q_0$  is the internal  $Q$  representing internal dissipation  $Q_i \sim 1/R_s$  where  $R_s$  is the surface resistance, and  $Q_c$ , sometimes called  $Q_{ex}$ , is the coupling  $Q$  representing dissipation to the external circuit and environment. The  $R$  in the equivalent circuit represents the power loss. The  $Q$ s add in reciprocal because losses are summed and  $1/Q$  is proportional to the losses. The  $Q_m$  of the circuit in Figure 2 is given by  $Q_m = R/\omega L$ .

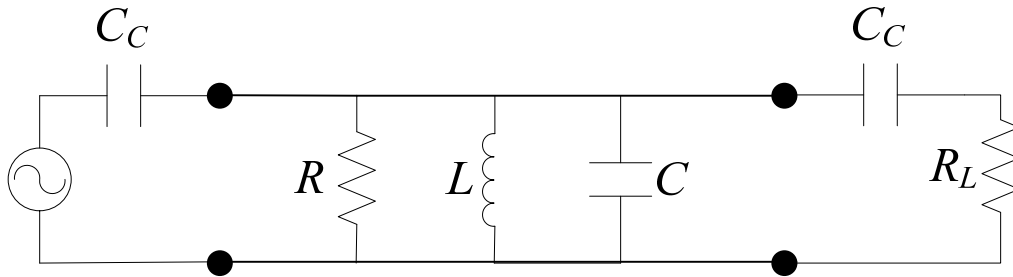


Figure 3. Equivalent circuit of a resonator coupled to a source and load.

Coupling the resonator to the external environment (circuit) is an essential consideration in order to drive the circuit and measure its properties. Figure 3 shows a two-port resonator with capacitive coupling to the external circuit. Inductive coupling is also possible. The coupling method used depends on the application. The frequency response for a two-port resonator is given by the usual Lorentzian function given in complex form by

$$S_{21}(f) = \frac{Q_m/Q_c}{1 + 2jQ_m(f - f_0)/f_0}, \quad (3)$$

where  $Q_m$  is the measured quality factor and  $f_0$  the resonance frequency. Resonators can also be measured in reflection mode in which case

$$S_{11}(f) = 1 - \frac{Q_m/Q_c}{1 + 2jQ_m(f - f_0)/f_0}. \quad (4)$$

where  $S_{ij}$  are the usual scattering parameters.

Some useful relationships are given in the following.

$$Q_i = \frac{Q_m Q_c}{Q_c - Q_m} = \frac{Q_m}{1 - 10^{-\frac{IL}{20}}}. \quad (5)$$

Where  $IL$  is the insertion loss defined as

$$IL = 20 \log S_{21} \quad (6)$$

Also

$$Q_i = Q_m \left( \frac{2}{S_{11} + S_{22}} \right) \quad (7)$$

One typically measures the magnitude and phase of Eq (4).  $|s_{21}|^2$  and  $\text{ang}(s_{21})$ .

$$|S_{21}|^2 = \frac{(Q_m/Q_c)^2}{1 + 4Q_m^2(f - f_0)^2} \quad (8)$$

$$\text{ang}(S_{21}) = \theta = \tan^{-1} 2Q_m(f - f_0) \quad (9)$$

These functions are plotted in Figure 4 for  $Q_m = Q_c = 1$

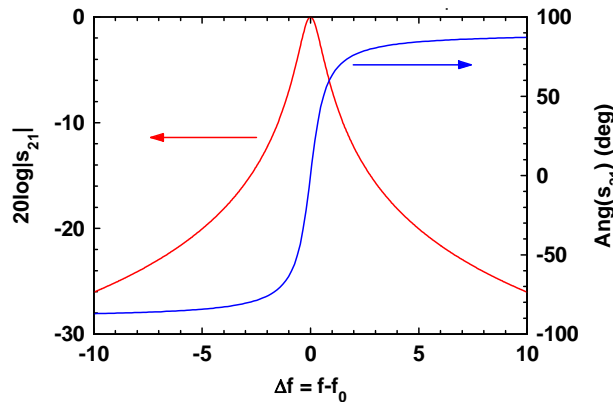


Figure 4 Magnitude and phase of the Lorentzian function. The magnitude is shown on a log scale.

The full width of the magnitude curve at one-half of the maximum value  $\mathcal{B}$  is related to the  $Q = f_0/\mathcal{B}$ . The slope of the phase at resonance is also equal to the  $Q$ .

The current circulating in a resonator is of importance for material evaluation discussed below. For a weakly coupled, transmission-line, two-port resonator as in Figure 3, the rms current  $I$  is given by (Oates, Anderson and Mankiewicz 1990)

$$|I| = \sqrt{\frac{r_v(1-r_v)4Q_i P}{\pi n Z_0}}, \quad (10)$$

where  $r_v$  is related to the insertion loss by  $IL = -20 \log r_v$ ,  $P$  is the power incident on the resonator,  $Z_0$  is the characteristic impedance of the transmission line and  $n$  is the overtone number.

## 1.2. Examples of planar superconducting resonators

Superconducting resonators are usually one of two types either planar, or three dimensional most often implemented as dielectric resonators. The simplest planar resonators are pieces of transmission line open or shorted at the ends one-half of the electromagnetic wavelength in length, so-called  $\lambda/2$  resonators. The kinds of transmission lines used are shown in Figure 5.

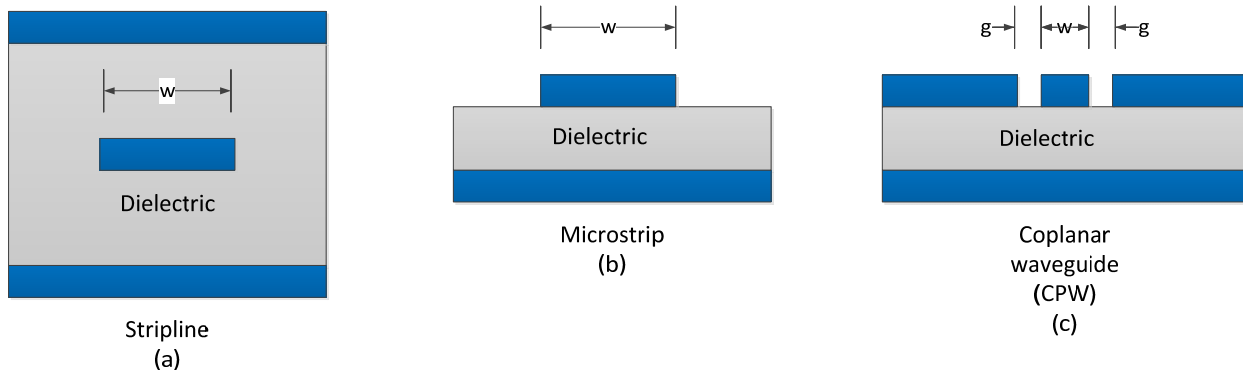


Figure 5 Examples of planar transmission-line-resonator geometries. (a) Stripline, (b) microstrip and (c) CPW.  $w$  is the width of the transmission line and  $g$  is the gap width for the CPW

The stripline geometry (left side of Figure 5) has ground planes above and below the center conductor and exhibits the highest  $Q$  values for transmission lines because the ground planes insure that radiation losses are minimized in this structure. The disadvantage is that three films are needed and the structure is often implemented with three substrates clamped together. Deposited dielectrics can also be used but are usually low  $Q$  and since the dielectric is part of the resonator, it lowers the  $Q$  of the resonator.

The middle of Figure 5 shows microstrip geometry. This has the advantage of needing only one substrate but deposition of films on both sides of the substrate is needed. The disadvantage of microstrip is that the lack of a ground plane above the patterned line allows extensive fringing fields to interact with the environment and limits the  $Q$  values attainable. This is only important when very high  $Q$ s ( $\sim 10^6$ ) are desired for instance for material evaluation. For filter structures, microstrip  $Q$ s are adequate, as discussed below.

The right side of Figure 5 shows the coplanar waveguide (CPW). CPW has several advantages: without the bottom ground plane it requires only one film; the width-to-gap ratio determines the impedance of the transmission line depending on the substrate relative dielectric constant  $\epsilon$  but independent of the substrate thickness. This can be implemented with or without the bottom ground plane and if the gap width is small compared to the substrate thickness the ground plane has no effect on the circuit. The CPW is most useful for narrow lines because as the gap width gets large, radiation losses become significant.

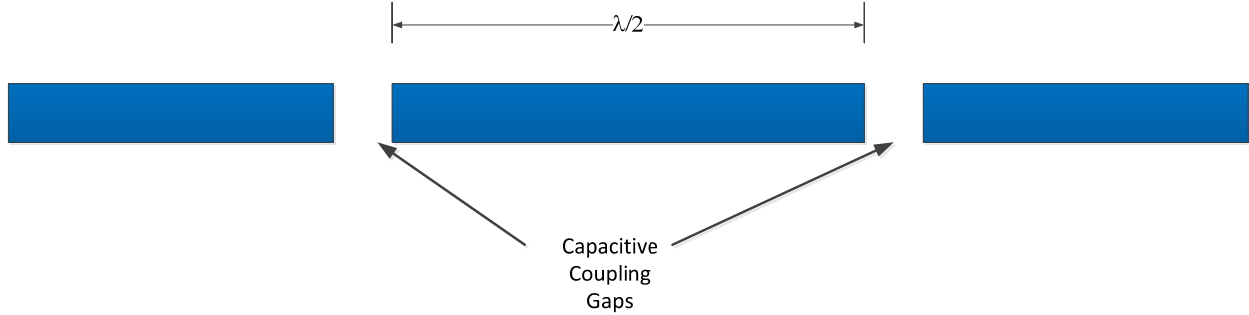


Figure 6  $\lambda/2$  distributed resonator in plan view

The simplest form of  $\lambda/2$  resonator is shown in Figure 6 in plan view. This corresponds to the equivalent circuit in Figure 3. It can be implemented in any of the three transmission geometries of Figure 5. The coupling to the resonator is achieved by a gap in the transmission line whose width determines the strength of the coupling and is usually treated as a capacitor in the circuit model. The strength of the coupling is adjusted to suit the particular application as discussed below. At very weak coupling such as with a small capacitance,  $Q_{ex} \gg Q_i$ , the line acts like an open circuited transmission line. At the fundamental resonance frequency  $f_0$  the transmission  $S_{21}$  is a maximum and far from resonance the  $S_{21}$  is small. The  $\lambda/2$  resonator also has overtone resonances at all integer multiples of the fundamental frequency, when the length of the resonator is multiples of  $\lambda/2$  that is  $n\lambda/2$ . Thus the resonator can be used to characterize the frequency dependence of the material parameters as discussed below.

To give an idea of the line sizes involved, the high-temperature-superconductor filters discussing in Section 3 use resonators of approximately 100- $\mu\text{m}$  to reach a characteristic impedance of about 50- $\Omega$  on the typical substrates used. The filters typically use a few  $\text{cm}^2$  generally less than 10 of substrate area.

Another common geometry is a feed line with a resonator or resonators coupled to the line as shown in Figure 7. Shown schematically is a capacitive coupling to the resonator using microstrip. The resonator can be  $\lambda/2$  in length if the far end of the resonator is open or  $\lambda/4$  if the end is shorted to ground, which is practical in CPW geometry but less easily implemented in microstrip or stripline. The response of the device is a dip at the resonance of the resonator

$$S_{21}(f) = \alpha \left( 1 - \frac{Q_m/Q_c}{1 + 2jQ_m(f - f_0)} \right) \quad (11)$$

where  $\alpha$  is the insertion loss of the feed line at frequencies near the resonance.

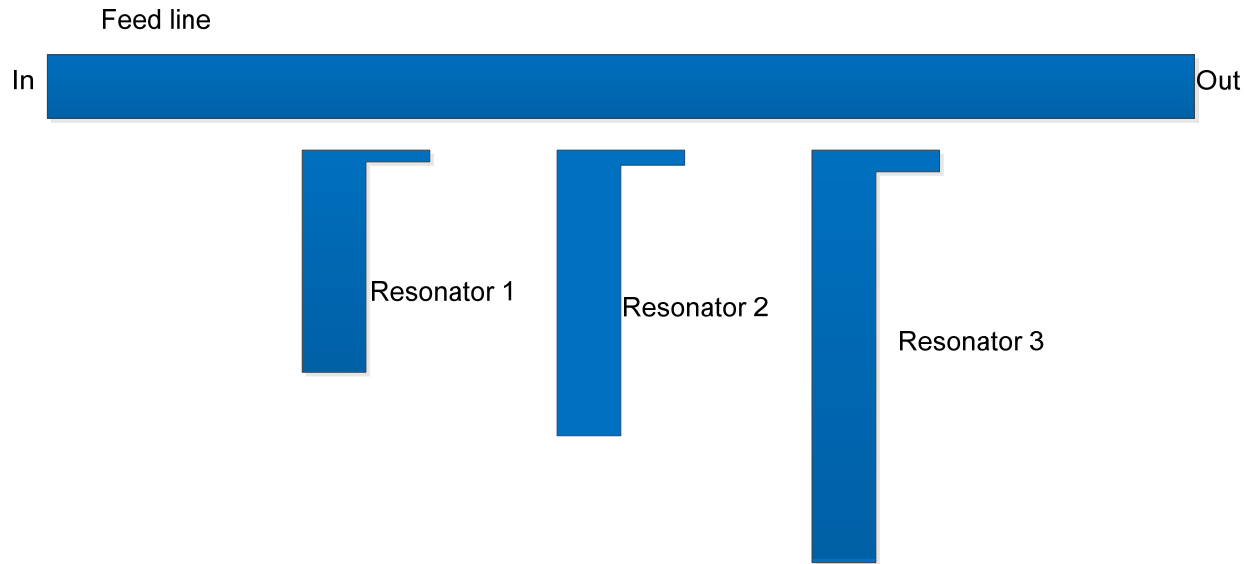


*Figure 7 Multiple resonators coupled to a feed line. This shows three resonators with different resonant frequencies. The  $S_{21}$  of the feedline would show three distinct dips.*

Multiple resonators can be coupled to a single feed line if the frequencies are separated more than a few resonance widths.

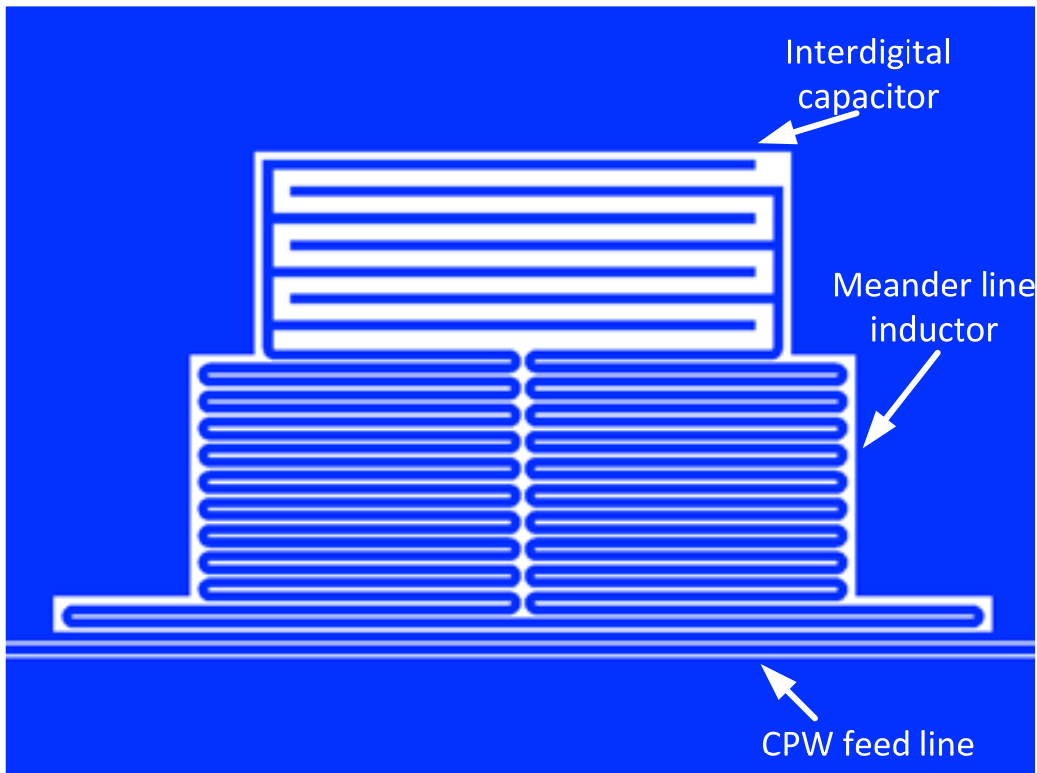


Figure 8 Example of quasi-lumped element resonator

In addition to the distributed resonators discussed above, so-called lumped element resonators have also been employed. The term lumped element is used because the resonator comprises separated inductor and capacitor. In superconducting resonators the implementation often is a miniature version in which the capacitor and inductor are combined in the same structure. Fig. 5 shows an example for CPW use. The resonator is shown coupled to a CPW feed line. At the top of the figure is the interdigital capacitor and below that is the meander line inductor. The use of lumped element resonators in superconducting filters is discussed later in this chapter.

### 1.3. Dielectric resonators

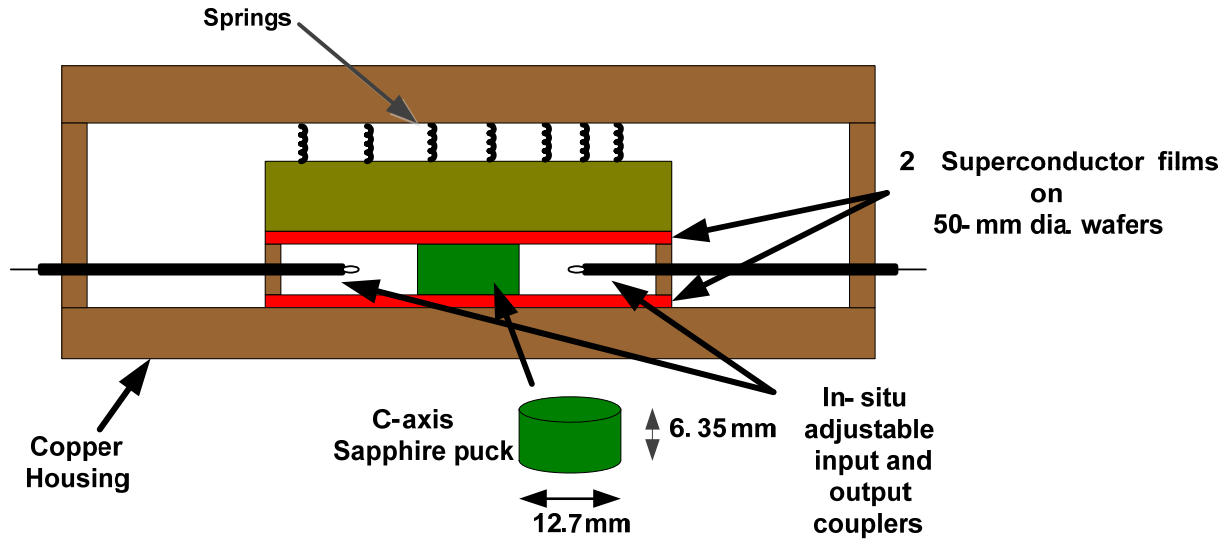


Figure 9 Dielectric resonator. Cross-section view. It contained in a copper housing and held together with springs as shown. The input and output couplers are adjustable while in the cryostat.

Dielectric resonators are three-dimensional cavities partially or fully filled with a low-loss dielectric material. Figure 9 shows one such example, a TE<sub>011</sub> mode resonator using single-crystal sapphire as the dielectric (Shen, Wilker, et al. 1992) (Xin, et al. 2000). Dielectric resonators are useful for superconductor material evaluation and for high-power superconducting filters as discussed below. The resonator shown can be analyzed as a dielectric-rod waveguide, one-half-wavelength long at resonance, and shorted on the two ends by the superconducting films as shown. Sapphire has extremely low loss at low temperatures and is a preferred material. The resonator is excited and the resonance detected by the loop antennas which serve as the input and output couplers. The coupling strength can be adjusted by moving the antennas closer or farther from the sapphire puck. The high relative dielectric constant of sapphire confines the energy in the puck so the fields in the puck and the currents induced in the end plates decay exponentially beyond the radius of the puck. Thus the interactions with the copper housing can be neglected. The frequency of the TE<sub>011</sub> mode as shown is 10.7 GHz. Typically, the resonator  $Q$  is determined by the ohmic losses in the superconductor due to the currents induced in the end films. The advantage of the dielectric resonator as shown is that for films thicker than a penetration depth the substrate on which the films are grown is not part of the cavity and does not contribute to the resonator  $Q$ . This is in contrast to the strip resonators shown in Figure 5, in which the substrate is part of the resonator cavity, so that the substrate for the film must be a low-loss material.

The TE<sub>011</sub> mode is most often used because it has the highest  $Q$  values of all the modes. Other modes such as the TM<sub>011</sub> can also be used. General discussion of dielectric resonators can be found in (Kajfez and Guillon 1986). The advantage of the dielectric resonator is that it uses unpatterned films and it is nondestructive. The films can be used in another device or context.

## 2. Applications of Superconducting resonators

### 2.1. Material evaluation

As discussed above the  $Q$  factor of a resonator is determined by the internal and external losses. If the external losses can be calibrated or minimized the resonator  $Q$  can be used to determine the losses of the

material used to fabricate the resonator, a transmission line for instance. The material losses can then be related to the surface resistance of the material, one of the fundamental material properties of the superconductor. In the two-fluid model the surface resistance  $R_s$  is given by

$$R_s = \frac{\omega^2 \mu_0^2 \lambda^3 \sigma_1}{2} \quad (12)$$

where  $\omega$  is the angular frequency ( $2\pi f$ ),  $\mu_0$  the free-space permeability,  $\lambda$  is the superconducting penetration depth,  $\sigma_1$  is the real part of the conductivity, and  $n$  is the total electron density. The  $Q$  of a transmission-line resonator is

$$Q = \frac{\omega L}{R} \quad (13)$$

where  $L$  is the inductance per unit length and  $R$  is the resistance per unit length of the transmission line. These values are dependent on the geometry of the line and are given by

$$L = \frac{\iint_A \mu_0 |H|^2 + \mu_0 \lambda^2 |J|^2 dA}{|I|^2} \quad (14)$$

and

$$R = \frac{\iint_A \frac{\sigma_1}{\sigma_2} |J|^2}{|I|^2} \quad (15)$$

where  $H$  is the magnetic field,  $J$  is the current density,  $I$  is the total current, and  $\sigma_2$  is the imaginary part of the conductivity.

$$\sigma_2 = \frac{1}{\omega \mu_0 \lambda^2} \quad (16)$$

The second term of the integral in Eq (14) is the kinetic inductance of the transmission line.

To calculate the surface resistance it is obvious that  $\lambda$  is needed. For new materials or new methods of fabrication the value of  $\lambda$  will not be known. The resonator can also be used to determine  $\lambda$  since it determines the kinetic inductance of the line. Since the  $f_0$  is given by

$$f_0 = \frac{1}{\sqrt{LC}}, \quad (17)$$

in principle  $\lambda$  could be determined by fitting the measured  $f_0$  using the equations for the capacitance and inductance of the transmission line. In practice this is a highly inaccurate way to determine  $\lambda$  due to fabrication tolerances of the resonator and the small values of the kinetic inductance. The practical

method is to measure  $f_0(T)$  whose changes are dominated by changes in the kinetic inductance. This method also requires assumption of a model for  $\lambda(T)$  for which the two-fluid model is most often employed.

$$\lambda(T) = \frac{\lambda(0)}{\sqrt{1 - \left(\frac{T}{T_C}\right)^4}} \quad (18)$$

Thus the procedure to determine the surface impedance of a superconductor is, 1) determine  $\lambda$  by measuring  $f_0(T)$ , fit the data using Eqs.(18) and (14), and then measure  $Q(T)$  from which the surface resistance is obtained.

Overtone resonances of the resonator can be used to measure  $R_S(\omega)$ . In a  $\lambda/2$  resonator the overtones occur at  $nf_0$  where  $n$  is an integer and in a  $\lambda/4$  resonator at  $nf_0$  where  $n$  is odd. If possible, for material evaluation it is best to use weak coupling. In that case the  $Q_m \approx Q_0$  and the analysis of the data is simple and accurate. Weak coupling increases the insertion loss however and signal to noise requirements may require stronger coupling.

A dielectric resonator can also be used to measure surface impedance. In such a resonator the superconducting end plates serve as ground planes and determine the resonator  $Q$ . This method has the advantage that the material does not need patterning and the measurements are nondestructive. The material can be used for other purposes following the characterization. If the film is thicker than  $2\lambda$  no knowledge of  $\lambda$  is needed to determine  $R_S$ .

Measurements of surface resistance with the dielectric resonator have been analyzed and found to be the most accurate determination the surface resistance (Mazierska and Wilker 2001). The dielectric resonator has been proposed as the international standard for measurement of surface resistance (International Electrotechnical Commission 2006).

## 2.2. Microwave Kinetic Inductance Photon Detectors

This application of superconducting resonators utilizes the change in kinetic inductance when a photon is incident on a superconductor. If the energy of the photon  $\hbar\omega$  is greater than the energy of the superconducting gap  $\Delta$   $\hbar\omega > \Delta$  then Cooper pairs are broken and the number of quasiparticles  $n_{qp}$  increases for a time  $\tau$  the recombination time for the quasiparticles to reform Cooper pairs. The kinetic inductance is given by

$$L_k = \mu_0 \lambda \quad (19)$$

and  $\lambda$  is related to the Cooper pair density by

$$\lambda = \sqrt{\frac{m}{\mu_0 e^2 n_s}} = \sqrt{\frac{m}{\mu_0 e^2 (1 - n_{qp})}} \quad (20)$$

From these considerations it can be shown (Day, et al. 2003) that the change in kinetic inductance  $\Delta L_k$  is given by

$$\Delta L_k \approx \frac{\delta n_{gp}}{2N_0\Delta} \quad (21)$$

where  $N_0$  is the density of states at the Fermi level. If the photons are absorbed by the material of the resonator, the change in inductance will change the resonance frequency of the resonator. Although the change is small, it can be readily observed when a superconducting resonator is used because of the very high  $Q$  factor possible with such a resonator. MKIDs are typically operated at  $<200$  mK.

From (16) it follows that the change in resonant frequency is given by

$$\frac{\Delta f}{f} = 0.5 \frac{\Delta L_k}{L} \quad (22)$$

where  $L$  is the total inductance of the equivalent circuit of the resonator.

For x-ray photons and typical circuit parameters  $\Delta f/f \approx 10^{-4}$ . The width of the resonance curve is

$$\frac{\delta f}{f} = \frac{1}{Q} \approx 10^{-5}. \quad (23)$$

Thus the shift in resonance frequency is larger than the width and use of a superconducting resonator allows easy detection of the induced frequency change. The detection can be made using the magnitude response Eq. (8) or phase response Eq. (9).

A major advantage of MKID detectors is the ability to fabricate arrays for imaging. The small size of the superconducting resonators makes this possible. Also clever multiplexing schemes have been developed to enable readout of multiple devices with only one output. The principle is similar to that discussed in the materials evaluation section above, in which many resonators are coupled to a single feed line. In the multiplexed MKIDs case the resonators are designed to have different resonant frequencies. Then the location of the radiation is identified with the resonator whose frequency has changed. Demonstration of hundreds of resonators each corresponding to one pixel in a focal plane array have been implemented.

A variety of superconducting materials (Szypryt, et al. 2015) have been used to make MKID devices including niobium, aluminum and the presently favored material niobium titanium. MKIDs can be used as detectors for millimeter wave, infrared, optical/UV, and x-ray photons. A detailed treatment is given in (Zmuidzinas 2012).

### 2.3. Applications of resonators in quantum information processing systems

A very new and exciting application of superconducting resonators is in quantum systems and specifically in quantum computing. These systems typically operate at temperatures  $<0.1$  K and incorporate superconductors and Josephson junctions (Devoret, Wallraff and Martinis 2004). The low temperatures open the possibility for superconductors other than niobium. Aluminum and titanium nitride are examples of the materials made useful by the low temperatures. (Oliver and Welander 2103). As Oliver and

Welanders discuss extensive use has been made of resonators to evaluate losses in materials. Interestingly the major source of loss at  $T < 0.1$  K is not the surface resistance of the superconductor but the so-called two-level systems (TLS).

Another important application of resonators is the readout of the quantum state of a qubit. (A qubit is the quantum analog of a binary bit.) Figure 10 shows one of the possible ways a resonator can be used to readout the state of the qubit shown. The qubit is a two state system and can be in either the state or superposition state as the result of manipulation or interaction with other qubits. The qubit is weakly coupled to the transmission line resonator but with enough strength that the state of the qubit changes the resonance frequency. In order to measure the state of the qubit, the resonator is interrogated with a CW microwave pulse. The measurement will result on one of the two states as required by quantum mechanics discriminated by measuring amplitude or phase of the transmitted signal. Superconductors are ideal for this application because the high  $Q$  gives a narrow linewidth making the discrimination with large signal-to-noise ratio possible and equally important the low loss of the resonator will not cause the decay of the qubit state to the ground state. There are many other applications of resonators in quantum systems even ones where the resonator becomes a quantum object with discrete energy states. Many applications also utilize the resonator with one microwave photon or less is in it.

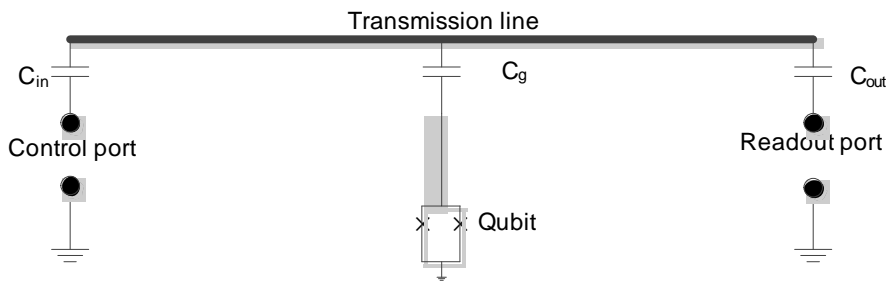


Figure 10 Resonator readout of a qubit after (Devoret, Wallraff and Martinis 2004).

### 3. Filters

#### 3.1. General considerations

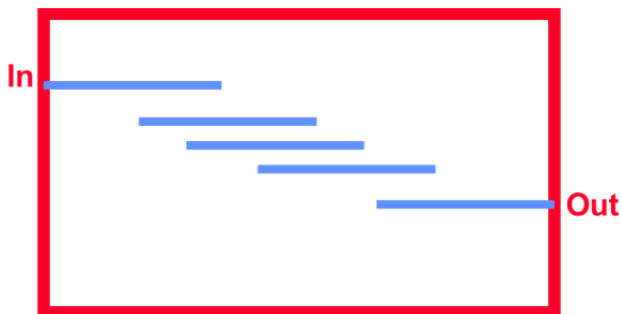


Figure 11 Schematic view of a microstrip filter with three coupled resonators, a 3-pole filter..

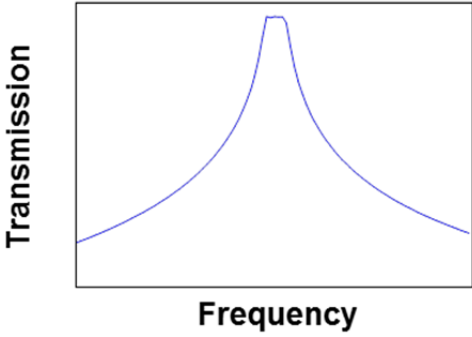


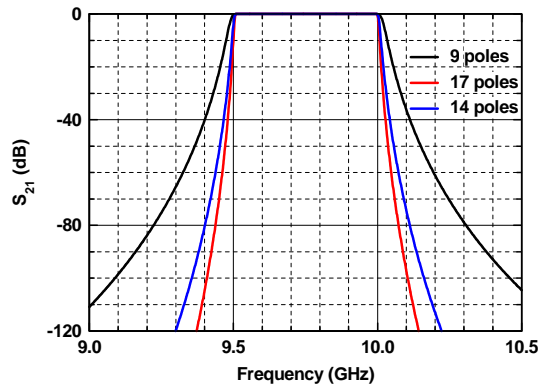
Figure 12 Schematic frequency response of the filter of Figure 11

The most common application of superconducting filters is as high-performance bandpass filters that are generally composed of resonators coupled together, thus the detailed discussion of resonators in the first parts of this article. Figure 11 shows a schematic of a coupled-resonator filter, in this case three resonators, and Figure 12 shows the frequency response expected for such a filter. High performance means: narrow passband,  $\sim 1\text{-}5\% \Delta f/f_0$  where  $\Delta f$  is the width of the passband of the filter and  $f_0$  is the center frequency of the passband; high selectivity with a sharp,  $< 1\%$  width, transition to out-of-band response; low insertion loss in the passband,  $< 0.5$  dB; and high out-of-band rejection,  $> 60$  dB. Superconductors are ideal for this application since resonators with extremely high Q factors, greater than  $10^5$  and low loss can be achieved in compact form in practical geometries such as microstrip or lumped element. The sharpness of the transition from passband to stop band is determined by the order of the filter, which is the same as the number of resonators coupled together to execute the filter. The order of the filter is numerically equal to the number of poles in the mathematical expression for the filter response, and thus filters of order  $n$  are often referred to as  $n$ -pole filters. Thus the filter depicted schematically in Figure 11 is a 3-pole filter.

The insertion loss of a coupled-resonator filter is given by

$$IL(\text{dB}) \sim \frac{n}{Q_u w}, \quad (24)$$

where  $n$  is the order of the filter, and  $w$  is the fractional bandwidth  $\Delta f/f_0$ . Since  $Q_u \sim 1/R_s$  the surface resistance, one sees that superconductors are advantageous for high-order filters. Figure 13 shows the



effects of filter order. Shown are calculations for an ideal filter using lossless resonators for a 5% fractional bandwidth, Chebyshev design (See (Pozar 1998) for details), for 9, 14, and 17-pole designs. The higher-order designs show a faster transition to the stopband from the passband of the filter.

Figure 13 Effects of filter order show are the frequency responses for ideal lossless 9, 14 ,and 17- pole filters of Chebyshev design.

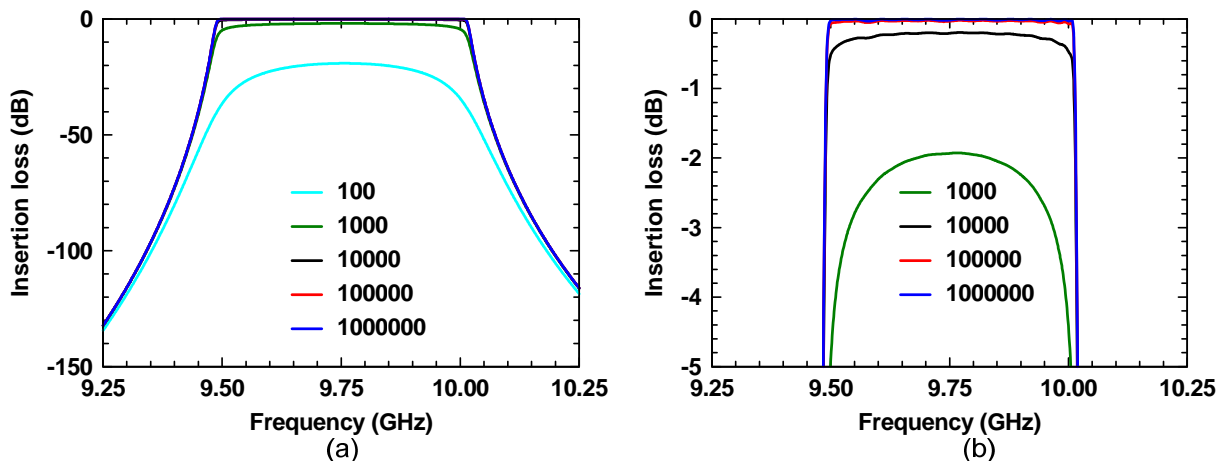


Figure 14 Effects of resonator  $Q$ . Filter insertion loss for a 14-pole filter for various values of the unloaded resonator  $Q$  as shown ranging from 100 to  $10^6$  (a) Insertion loss on a course scale. (b) Insertion loss on an expanded scale showing the detail of the passband. In this view the loss of the filter with  $Q = 100$  is off the visible scale.

Figure 14 shows the effects of finite unloaded  $Q$  values of the resonators. Part (a) shows the responses of a 14-pole filter for various values of the resonator  $Q$  factors on a course scale, while (b) shows the same results on an expanded scale. One sees that for  $Q$  factors less than about 1000 the insertion loss becomes quite large and the sharp roll off at the passband edges is degraded. Use of conventional materials such as copper in microstrip resonators produces  $Q$  factors of approximately 100 and cannot compete with superconductors for high performance.

In applying a superconducting filter or indeed a filter of any kind, first one must specify the bandwidth and the level of rejection at some frequency outside of the band of interest. As shown in Figure 13 , the level of rejection needed at a specific frequency specifies the order of the filter. Once the bandwidth and filter order are determined, one must synthesize the filter, meaning compute the frequencies and coupling of the resonators. The synthesis takes into account also the flatness of the passband. Then the resonators are designed, distributed, or lumped element for example, and the coupling coefficients needed are also designed knowing the geometry of the resonators.

The design of microstrip filters is discussed in Hong and Lancaster (Hong and Lancaster 2001) and Pozar (Pozar 1998). A thorough treatment of lumped-element designs is given in (Chaloupka and Kolesov 2001). The filter response is determined by the strength of the coupling between resonators. In most conventional designs the coupling is only to the adjacent resonators; that is resonator  $n$  is coupled only to resonators  $n-1$  and  $n+1$ . Design details for calculating coupling strengths are given in (Hong and Lancaster 2001) and (Pozar 1998). Of course the desired coupling strengths in the fabricated filter are determined by the geometry used for the implementation of the filter.

Distributed resonators, such as transmission line resonators, exhibit overtone responses at multiples of the fundamental frequency. Filters designed with such resonators therefore have spurious out-of-band responses at those overtone resonances. In many cases this limits the possible out-of-band rejection for these designs. Lumped elements alleviate this problem as discussed in the below.

The discussion so far has considered so called “all pole” filters. These exhibit a response that is a mathematical function that contains only poles. An even narrower transition to out-of-band response (faster fall-off) can be obtained if the mathematical function describing the response contains zeros as well as poles. This is called an elliptical or quasi-elliptical filter. Details are discussed in (Hong and Lancaster 2001).

Band-reject filters also called band-stop and notch can be designed using a similar synthesis and design process. See Hong and Lancaster for details.

A variety of different designs have been used to implement filters. The chapter on microwave resonators and filters in the first edition of this Handbook (Z.-Y. Shen 2003) discusses several examples so the details need not be repeated here. As examples from the first edition, distributed resonators such as the half-wave resonators as shown schematically in Figure 11 have been often employed. Figure 15 is an example of an actual layout from the first edition. Another design example is a so called hair-pin resonator as discussed the first edition shown in Figure 16 .

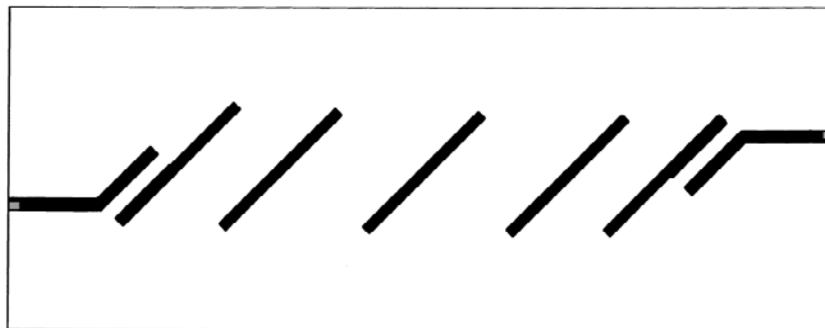


Figure 15 X-band 5-pole filter From (Z.-Y. Shen 2003)the lines are approximately 160- $\mu$ m wide



Figure 16 Hairpin resonators From (Z.-Y. Shen 2003) Linewidths are approximately  $160 \mu m$

A review of superconducting filters would not be complete without an example of a well-designed and fabricated filter. Figure 17 shows an example of the response of high-order HTS filters intended for use in wireless communication systems (Tsuzuki, Suzuki and Sakakibara 2000) Part (a) is a 16-pole filter and (b) is a 32-pole filter. Both plots show  $S_{21}$  and  $S_{11}$ .

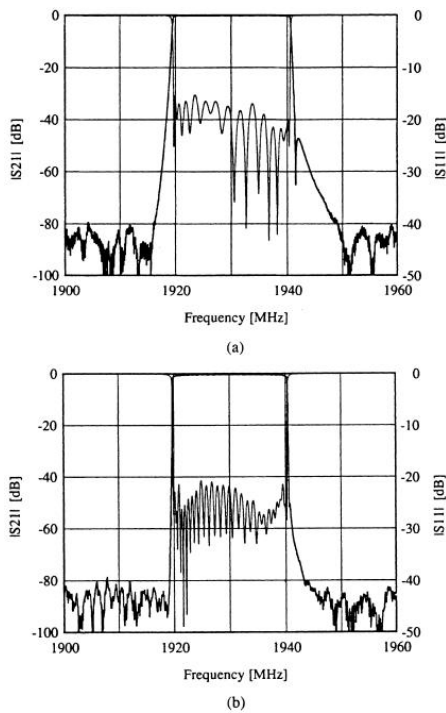


Figure 17 Examples of filter responses. (a) 16-pole filter and (b) 32-pole filter (Tsuzuki, Suzuki and Sakakibara 2000)

The first edition of this Handbook considered only HTS YBCO filters, and subsequent filter development has also been with YBCO as the superconductor. Later in Section 3.4 LTS filters are introduced. Since the publication of the first edition some of the recent developments have been in miniaturization through the use of lumped element designs. Lumped elements do not have the same overtone responses as distributed

microstrip designs. Wang et al. (Wang, et al. 2013) have demonstrated a very wide stopband for a UHF filter with the first spurious frequency at 5.2 times the fundamental  $f_0$  by using lumped elements.

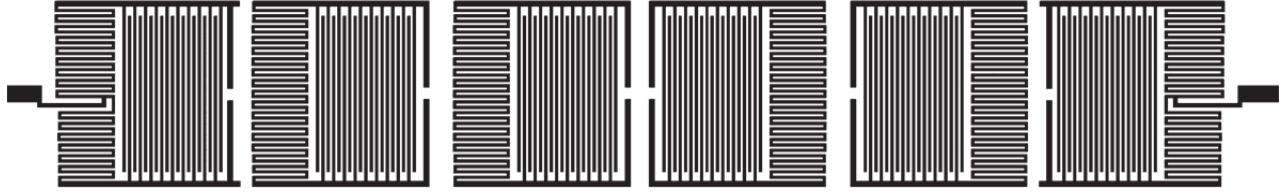


Figure 18 Layout of lumped element resonators to implement the filter shown in Figure 19 (Wang, et al. 2013)

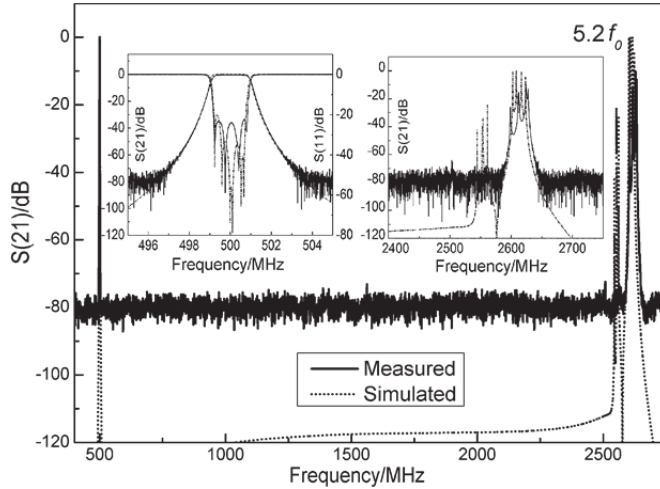


Figure 19 Response of the filter whose layout is shown in Figure 18. The first spurious response at 5.2 times the fundamental is very far from the fundamental leading to a very wide stopband.

### 3.2. Applications of filters

The application that has seen the most success for applying superconducting filters is at the front end of RF receiver systems (B. Willemsen 2001) (B. A. Willemsen 2001). The layout of the receiver front end is shown in Figure 20. The filter is designed to pass only the desired signals and to reject interference from nearby sources at frequencies close to the desired frequency. This is especially valuable in today's crowded frequency spectrum in which most wireless communication systems operate. The low loss allows placement of the filter in front of the low noise amplifier to protect the amplifier from large out-of-band signals that could produce nonlinear behavior of the amplifier but the low insertion loss insures that the noise figure of the system will not be compromised. The conventional design places the filter after the low-noise amplifier leaving the LNA open for overload or nonlinear behavior. The noise figure of the receiver is set by the front end and determines the sensitivity of the receiver to small signals. The noise figure in dB of the superconducting filter is given by

$$F_{\text{dB}} = 10 \log \left( 1 + (IL - 1) \frac{T}{290} \right) \quad (25),$$

where  $IL$  is the insertion loss of the filter and  $T$  is the temperature.

Another application is for radio astronomy receivers where the front end is already operated at cryogenic temperatures. One such filter is described in (Zhou, et al. 2005).

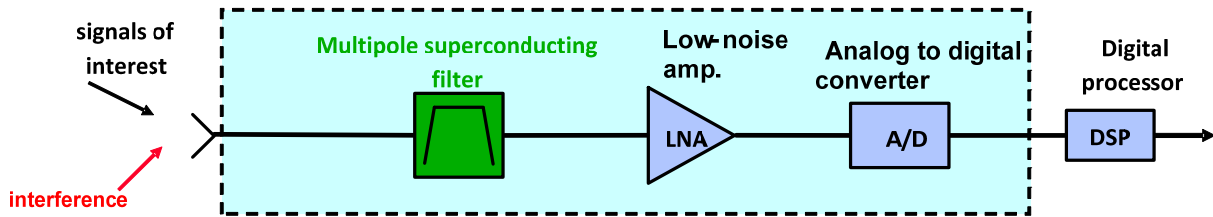


Figure 20 Receiver front end with a superconducting filter. The superconducting filter removes interference that could overload the LNA, but does not degrade the noise figure.

### 3.3. Nonlinear effects and power handling.

Because of the finite current carrying capability of superconductors (critical current) the amount of power that a superconducting filter can transmit is limited. The exact limitation is dependent on the geometry, the filter order, and the fractional bandwidth. For microstrip designs the power limitation is about 100 mW or less. In any kind of a strip resonator (Figure 5) the current distributions peaked at the edge of the line (See (Van Duzer and Turner 1999) and (Sheen, et al. 1991)). When the inhomogeneous current distribution of microstrip lines is taken into account, the power limitation usually corresponds approximately to the power level at which the microwave current exceeds the DC critical current at the places where the current density is the highest. There are, however, subtle differences between RF and DC critical currents (D. E. Oates 2007). Power handling of 100 mW is sufficient for RF front-end applications discussed above. However, for transmitter applications the 100 mW power handling is not sufficient. Attempts at increasing the power handling have been undertaken. Some used wider lines or multiple lines on microstrip, but these are still limited to less than 1 W. The best efforts have usually employed variations of the dielectric resonator discussed above in this chapter. An example has shown more than 70 W in a three-pole .79%-bandwidth design (Anderson, et al. 1999). Another variation of the disk resonator design was shown to produce 42 W power handling (Kato, et al. 2015) The variations of the disk resonator all rely on the more homogeneous current distribution and the lack of sharp peaks in the current density to increase the power handling.

The power handling is governed by a critical current that when exceeded produces a sharp increase in surface resistance and a collapse of the filter transfer function. However even at low currents nonlinear effects can occur and while not influencing the filter transfer function can produce intermodulation distortion (IMD). The nonlinearity results from either the breaking of cooper pairs (nonlinear Meissner effect) or in weak links at the grain boundaries of the film material, both of which lead to a nonlinear surface impedance. The physics and origins of the nonlinearity are discussed in (D. E. Oates 2007). It is an effect that needs consideration in superconducting filters but of course is absent in conventional filters. IMD results from the mixing of two tones  $f_1$  and  $f_2$  due to the nonlinear impedance. The third-order mixing products at  $2f_1-f_2$  and  $2f_2-f_1$  fall in the passband of the filter and are spurious signals that distort the filter response. Figure 21 shows the measured IMD for a YBCO resonator. Shown is the power out vs power in for the fundamental frequency and one of the two third order intermodulation products on a log plot. The fundamental is linear (slope one in the log plot) in the input power until saturation is reached. The third order IMD product because it is a third order effect depends on the cube of the input power and

exhibits a slope of three in the plot. The size of the IMD is strongly dependent on the material. LTS films have lower IMD than the HTS because of the basic physics of the superconductivity being different.

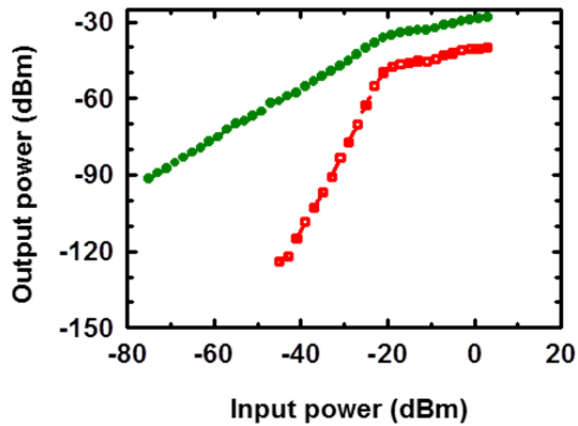


Figure 21 An example of IMD in a YBCO superconducting resonator at 77 K. The  $f_0$  of the resonator is 1.5 GHz. The green points are the fundamental frequency and increase linearly with the input power until saturation. The red points are the third-order IMD resulting from two tones within the bandwidth of the resonator.

A thorough analysis of the effects of nonlinearities in superconducting devices has been given in (Collado, Mateu and O'Callaghan 2005).

### 3.4. Future trends in filters

Almost all of the filter development work and applications to date have been with the use of HTS, as noted above. YBCO is the overwhelming material of choice for the applications studied. Because the fabrication of YBCO with low microwave losses and good power handling entails single-crystal-like epitaxial films, and because of the necessity of epitaxy, multilayer fabrication processes have not been practical. For this reason filter designs are limited to those that can be implemented in a single superconducting layer. The epitaxy also requires expensive single-crystal substrates and when required in diameters typical of modern electronic circuit fabrication (200-mm diameter) cost becomes prohibitive.

Multilayer processes have been developed specifically for LTS digital circuits. See for example (HYPRES Inc. 2012) and (Tolpygo, et al. 2015). These processes have four and eight niobium layers, respectively. They can be adapted for passive filter circuits. While these LTS multilayer circuits have not yet been extensively utilized, it is likely that such applications will grow in the future. The multilayers allow for more design flexibility than the single layer for the HTS filters. For example lumped element filters with spiral inductors can be used, which are much more compact than the meander line inductors required in the single-layer designs. Also stronger values of coupling between resonators are available because of the possible use of broadside coupling between layers. This is important for wideband filters. Lumped elements also avoid the problem of overtone resonances in transmission-line resonators. Highly miniature filters using the Hypres process have been reported (Setoodeh, Laforge and Mansour 2011). The intended application is as the interference rejection filter in front of a superconducting analog-to-digital converter (ADC).

The best systems for applications of the LTS passive devices will most likely be systems that are already operating at cryogenic temperatures. For example high-speed ADC or in quantum information processing systems alluded to in Sec. 2.3

Tunable filters are a sought-after goal. A tunable filter with rapid electronic tuning that maintains constant bandwidth and low loss and undistorted passband over an octave or so is desirable. There are applications for tunable bandpass and band-reject filters. Electronically tunable filters have been investigated using various means to change the center frequency. Tuning with variable permeability using ferrites, variable permittivity using ferroelectrics, variable capacitance using semiconductor varactor diodes and micromechanical MEMS elements have been investigated. It is safe to say that no technology has proven entirely satisfactory. This search for an effective tunable filter will continue.

#### 4. Summary

As presented here applications of resonators and filters have grown in the last decade. Although application of HTS filters in wireless systems has not been widely adapted, research and field trials of HTS filters have continued. Other niche applications are occurring. However the applications that have grown the most in the last decade are at low temperatures using LTS superconductors as has been presented here. This field is growing fueled in part by the growth in quantum information systems. A topic for instance that is just emerging is the use of resonators to implement low noise quantum limited amplifiers.

#### 5. Citations

Anderson, Alfredo C, et al. "Transmit filters for wireless basestations." *IEEE Transactions on Applied Superconductivity*, 1999: 4006-4009.

Chaloupka, H J, and S Kolesov. "Design of lumped-element 2D RF devices." In *Microwave superconductivity*, edited by H Weinstock and M Nisenoff, 205-238. Dordrecht, Netherlands: Kluwer Academic Publishers, 2001.

Collado, Carlos, Jordi Mateu, and Juan M O'Callaghan. "Analysis and Simulation of the Effects of Distributed Nonlinearities in Microwave Superconducting Devices." *IEEE Transactions on Applied Superconductivity* 15, no. 1 (2005): 26-39.

Day, Peter K, Henry G LeDuc, Benjamin A Mazin, Anastasios Vayonakis, and Jonas Zmuidzinas. "A broadband superconducting detector suitable for use in large arrays." *Nature* 425 (2003): 817-821.

Devoret, M H, A Wallraff, and J M Martinis. "Superconducting Qubits: A Short Review." *arXiv:cond-mat/0411174v1*, 2004: 1-41.

Hong, Jia-Sheng, and Michael J Lancaster. *Microwstrip filters for RF/microwave applicattions*. New York, NY: John Wiley and Sons, 2001.

HYPRES Inc. "Design rules." 2012.

- International Electrotechnical Commission. *Electronic characteristic measurements –Surface resistance of superconductors IEC 61788-7 at microwave frequencies*. Geneva Switzerland: International Electrotechnical Commission, 2006.
- Kajfez, Darko, and Pierre Guillon. *Dielectric Resonators*. Dedham, MA: Artech House Inc., 1986.
- Kato, Tomoki, Atsushi Saito, Ryota Tsurui, Hidekazu Teshima, and Shigetoshi Ohshima. "Power-Handling Capability of Superconducting Filters Using Disk- and Ring-Type Bulk Resonators." *IEEE Transactions on Applied Superconductivity* 25, no. 3 (2015): 1501105.
- Mazierska, Janina, and Charles Wilker. "Accuracy Issues in Surface Resistance Measurements of High Temperature Superconductors Using Dielectric Resonators." *IEEE Transactions on Applied Superconductivity* 11, no. 4 (2001): 4140-4147.
- Oates, D E, A C Anderson, and P M Mankiewich. "Measurement of the surface resistance of YBa<sub>2</sub>Cu<sub>3</sub>O<sub>7-x</sub>." *Journal of Superconductivity* 3, no. 3 (1990): 251-259.
- Oates, Daniel E. "Overview of nonlinearity in HTS: what we have learned and prospects for improvement." *Journal of Superconductivity and Novel Magnetism* 20 (2007): 3-12.
- Oliver, William D, and Paul B Welander. "Materials in superconducting quantum bits." *MRS Bulletin* 38 (2103): 818-825.
- Pozar, David M. *Microwave Engineering*. New York, NY: John Wiley and Sons, Inc., 1998.
- Setoodeh, Sormeh, Paul D Laforge, and Raafat R Mansour. "Realization of a highly miniaturized wideband bandpass filter at the UHF band." *IEEE Transactions on Applied Superconductivity* 21, no. 3 (2011): 538-541.
- Sheen, David M, Sami M Ali, Daniel E Oates, Richard S Withers, and J A Kong. "Current distribution, resistance, and inductance for superconducting strip transmission lines." *IEEE Transactions on Applied Superconductivity* 1, no. 2 (1991): 108.
- Shen, Z\_Y, Charles Wilker, Philip Pang, William L Holstein, Dean Face, and Dennis J Kountz. "High T, Superconductor-Sapphire Microwave Resonator with Extremely High Q-Values up to 90 K." *IEEE Transactions on Microwave Theory and Techniques* 40, no. 12 (1992): 2424.
- Shen, Z-Y. "Microwave resonators and filters." In *Handbook of Superconducting Materials*, edited by David A Cardwell and David S Ginley, 1716-1725. Bristol, UK: Institute of Physics Publishing, 2003.
- Szypryt, P, B A Mazin, B Bumble, H G LeDuc, and L Baker. "Ultraviolet, Optical, and Near-IR Microwave Kinetic Inductance Detector Materials Developments." *IEEE Transactions on Applied Superconductivity* 25, no. 3 (2015): 2400604.
- Tolpygo, S K, V Bolkhovsky, T J Weir, L M Johnson, M A Gouker, and W D Oliver. "Fabrication process and properties of fully-planarized deep-submicron Nb/Al-AlO<sub>x</sub>/Nb Josephson junctions for VLSI circuits." *IEEE Transactions on Applied Superconductivity* 25, no. 3 (2015): 1100906.

- Tsuzuki, Genichi, Masanobu Suzuki, and Nobuyoshi Sakakibara. "Superconducting filter of IMT-2000 Band." *IEEE Transactions on Microwave Theory and Techniques* 48, no. 12 (2000): 2519-2525.
- Vaglio, Ruggero. "RF superconducting cavities for accelerators." In *Microwave Superconductivity*, edited by Harold Weinstock and Martin Nisenoff, 447-472. Dordrecht, Netherlands: Kluwer Academic Publishers, 2001.
- Van Duzer, Theodore, and Charles W Turner. *Principles of superconductive devices and circuits*. Second. Upper Saddle River, NJ: Prentice Hall PTR, 1999.
- Wang, Jingchen, Bin Wei, Bisong Cao, Xiaoping Zhang, Xubo Guo, and Xiaoke Song. "A UHF-Band Narrow-Band HTS Bandpass Filter With Wide Stopband Using Interdigital Structure." *IEEE Transactions on Applied Superconductivity* 23, no. 6 (2013): 1502108.
- Willemsen, B A. "HTS wireless applications." In *Microwave Superconductivity*, edited by Harold Weinstock and Martin Nisenoff, 387-416. Dordrecht, Netherlands: Kluwer Academic Press, 2001.
- Willemsen, Balam. "HTS filter subsystems for wireless telecommunications." *IEEE Transactions on Applied Superconductivity*, 2001: 60-67.
- Xin, Hao, Daniel E Oates, A C Anderson, R L Slattery, G Dresselhaus, and M S Dresselhaus. "Comparison of Power Dependence of Microwave Surface Resistance of Unpatterned and Patterned Unpatterned and Patterned." *IEEE Transactions on Microwave Theory and Techniques* 48, no. 7 (2000): 1221-1226.
- Zhou, Jiafeng, Michael J Lancaster, Frederick Huang, Neil Roddis, and Dave Glynn. "HTS narrow band filters at UHF band for radio astronomy applications." *IEEE Transactions on Applied Superconductivity*, 2005: 1004-1007.
- Zmuidzinas, Jonas. "Superconducting microresonators: physics and applications." *Annual Review of Condensed Matter Physics* 3 (2012): 169-214.